

## Local electronic structure and luminescence properties of Er doped ZnO nanowires

Juan Wang, M. J. Zhou, S. K. Hark, and Quan Li<sup>a)</sup>

*Department of Physics, The Chinese University of Hong Kong, Shatin, New Territory, Hong Kong*

D. Tang

*FEI Company, 5600KA Eindhoven, Netherlands*

M. W. Chu and C. H. Chen

*Center for Condensed Matter Sciences, National Taiwan University, Taipei 106, Taiwan*

(Received 9 July 2006; accepted 20 October 2006; published online 30 November 2006)

Using combined microscopy and optical characterizations, the authors demonstrate effective Er doping into freestanding ZnO nanowires via ion implantation. The Er atoms are observed to take the substitutional sites in ZnO without causing obvious distortion to the host lattice. While the band gap threshold of the Er doped ZnO nanowires remains similar to that of the undoped ZnO, band tail states are created in the band structure of the ZnO upon Er doping. Room temperature 1.54  $\mu\text{m}$  emission is achieved in the doped nanowire sample after oxygen annealing. In particular, the generation of the band tail state(s) in the band gap of the ZnO nanowire host is found to be responsible for the 1.54  $\mu\text{m}$  emission under the below-band-gap indirect excitation. © 2006 American Institute of Physics. [DOI: 10.1063/1.2399340]

Recent successes in nanowire synthesis and assembly, especially the prototype device demonstrations using the bottom-up approach, arouse increasing interests in these pseudo-one-dimensional (1D) nanomaterials.<sup>1</sup> With the phase pure nanowire synthesis becoming controllable, nanowire doping for desired electrical, magnetic, and/or optical properties becomes one of the current focuses of intense research efforts. Although doping induced electronic structure change is expected to play an important role in determining various properties of these 1D nanomaterials,<sup>2,3</sup> limited amount of direct experimental evidence is available addressing such an issue.<sup>4</sup>

Er doping into various semiconducting materials is of continuous interests due to its effective 1.54  $\mu\text{m}$  emission for applications in the optical communications.<sup>5,6</sup> Numerous studies of Er doped ZnO thin films<sup>7–10</sup> suggest that the 1.54  $\mu\text{m}$  luminescence, being characteristic of the Er intra-4*f* transitions, would occur when the Er atoms are triply ionized and embedded in the ZnO hosts, allowing an effective energy transfer from the excited host electrons in the conduction band to the Er ions—a common indirect excitation mechanism for Er doped semiconductors.<sup>5</sup> Nevertheless, little is known when such doping takes place in nanowires—freestanding single crystals with large surface/volume ratio, as compared to its bulk or thin film counterparts. The dopant sites, doping induced defects, and especially the possible host electronic structure change upon doping are expected to have important impacts on the optical properties of these nanowires and thus are of the main interests in the current study.

In the present work, we report doping of Er into the ZnO nanowires using a metal ion implantation system followed by annealing in an oxygen environment, resulting in effective 1.54  $\mu\text{m}$  emission of these nanowires. We inspect both the microstructure and the electronic structure change of the ZnO nanowire host at the dopant sites. The luminescence

mechanism and the effect of the dopant induced electronic structure change on the 1.54  $\mu\text{m}$  emission are discussed.

The ZnO nanowires were synthesized by thermal evaporation of ZnO and carbon powder mixture with 1/1 ratio, using a high temperature vacuum tube furnace.<sup>11</sup> The as-synthesized nanowires (with an average diameter of 40 nm and a diameter distribution of  $\pm 20$  nm) were then dispersed onto a graphite substrate to form a thin layer of nanowire film [Fig. 1(a)] before Er ion implantation using a metal vapor vacuum arc system.<sup>12</sup> The ion incident direction is perpendicular to the substrate surface. The implantation energy was chosen at 50 keV in order to compromise the requirements on the implantation depth and the implantation damage minimization. The ion dose was controlled at  $5 \times 10^{15} \text{ cm}^{-2}$ . After Er ion implantation, part of the ZnO nanowires was transferred to another furnace for oxygen annealing at 800 °C for 1 h.

The microstructure of the samples was examined using various transmission electron microscopy (TEM, Tecnai G2 microscope)-related techniques. The local chemical compositions of the nanowires were investigated using energy dispersive x ray (EDX, Oxford Instrument) performed in the scanning transmission electron microscope (STEM) probe mode, with a probe size of  $\sim 3$  nm. The electronic structures of individual nanowires were investigated using electron energy loss spectroscopy (EELS), using a Gatan imaging filtering system, attached to the same microscope. The energy loss spectra (instrumental resolution of 0.15 eV with monochromator on) were taken at a small momentum transfer, and direct deconvolution<sup>13</sup> was performed to remove multiple scattering and generate the loss functions.<sup>14</sup> The cathodoluminescence (CL) measurements were carried out using a MonoCL system with an excitation power at 20  $\mu\text{W}$  (Oxford Instrument) in a scanning electron microscope (SEM). The photoluminescence (PL) of the doped nanowires was measured using both the 325 and the 442 nm line of a He–Cd laser.

The general morphologies of the ZnO nanowires before and after ion implantation are similar, as disclosed by the

<sup>a)</sup> Author to whom correspondence should be addressed; electronic mail: liquan@phy.cuhk.edu.hk

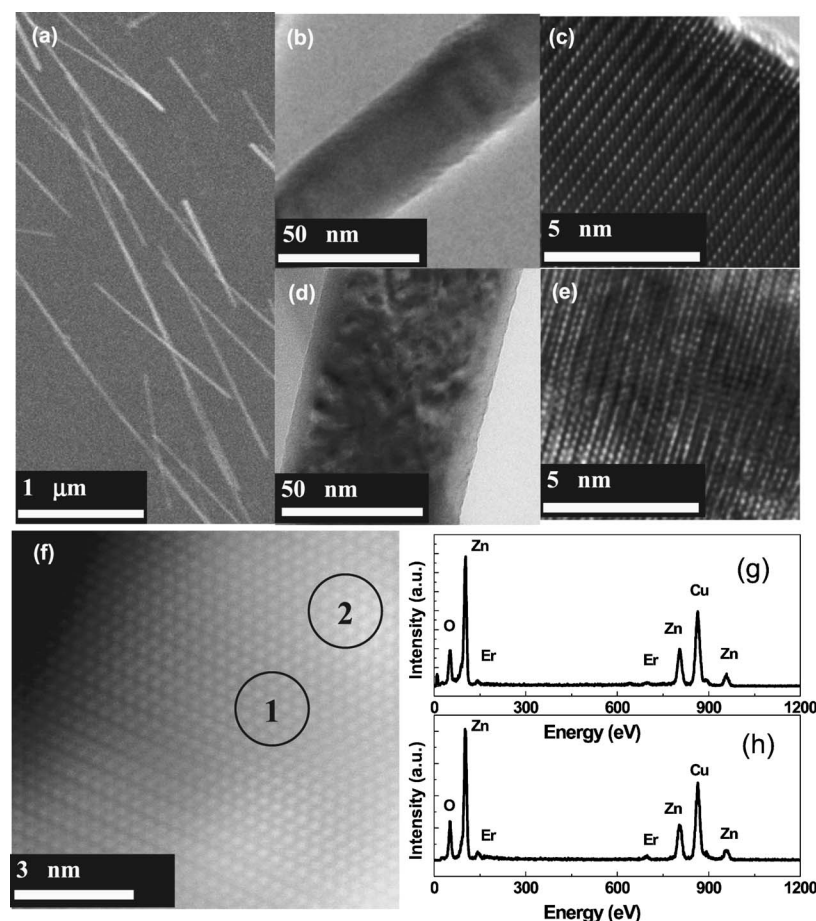


FIG. 1. (a) SEM image of the ZnO nanowires dispersed on the substrate before ion implantation. (b) Low magnification TEM image of the ZnO nanowire before ion implantation. (c) The corresponding high resolution electron microscopy (HREM) image of nanowire in (b). (d) Low magnification TEM image of ZnO after Er ion implantation (annealed). (e) The corresponding HREM image of nanowire in (d). (f) High resolution STEM image of the Er doped ZnO nanowire (annealed). (g) EDX spectrum taken from region with darker contrast [marked as 1 in (f)]. (h) EDX spectrum taken from region with brighter contrast [marked as 2 in (f)].

bright field TEM images [Fig. 1(b)–1(e)]. Although obvious light/dark contrast can be observed in the nanowires after the Er implantation, suggesting strain and/or mass-thickness difference in the corresponding regions, lattice defects of either line or plane type are seldom detected in these nanowires. Visualization of Er incorporation into the ZnO lattice is realized using STEM-EDX, by which the correlation between the local microstructure and the chemical composition can be established.<sup>15</sup> The high resolution STEM image in Fig. 1(f), which is taken from the Er doped ZnO nanowire (annealed), reveals the structure intactness of the nanowire host and the possible Er residing site. By focusing the electron probe on the regions [as marked by circles 1 and 2 in Fig. 1(f)] of darker and brighter contrasts, we found that the local Er concentration varies from <1% in the darker region to ~3% in the brighter region, respectively.

Although microstructure intactness of these doped nanowires is suggested by the TEM (STEM) study, doping via ion implantation indeed leads to defect generation in the nanowire host. CL taken from the as-implanted nanowires discloses significantly reduced band edge emission and a high-intensity green luminescence band (Fig. 2). The broad green luminescence is normally interpreted as originating from the ZnO native point defects (such as O vacancies) forming deep levels in its band structure,<sup>16</sup> which is expected during the highly nonequilibrium doping process. On the other hand, substituting  $\text{Er}^{3+}$  for  $\text{Zn}^{2+}$  naturally requires the generation of O defects in order to maintain the charge neutrality. Such structure degradation is partially recoverable via oxygen annealing, which leads to increased band edge emission and decreased green emission. However, full recovery to that of the original ZnO nanowire is not possible even with pro-

longed annealing process. In fact, such partial recovery is reasonable when considering charge neutrality argument as stated earlier.

Similar band tail state(s) as those revealed by the CL spectra are(is) also observed in the EELS study of the doped ZnO nanowire. The loss functions ( $\text{Im}[-1/\epsilon]$ ) of both the as-synthesized and the doped (annealed) ZnO nanowire are shown in Fig. 3. While most of the features in the loss functions of both samples, including the band gap, the interband transitions, and the bulk plasmon oscillation, resemble those of the bulk ZnO,<sup>17,18</sup> a broad defect band with energy ranging from 2 eV to the band edge is visible. In addition, an extra peak at ~1.4 eV is also detected in the doped ZnO nanowire. Although its origin is not clear at this stage, we find that the excitation energy (~1.4 eV) differs from that of the commonly reported O-related defect state(s) (~2.4 eV).<sup>16</sup> In addition, no clear trend is found in the oscillator strength change of such transition before and after

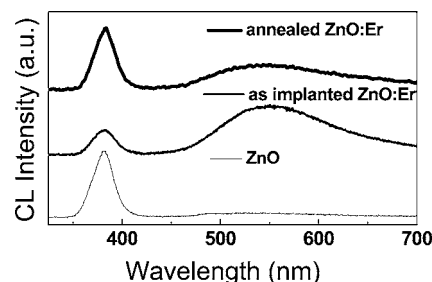


FIG. 2. Cathodoluminescence spectra of the ZnO nanowires before and after ion implantation, and after annealing.

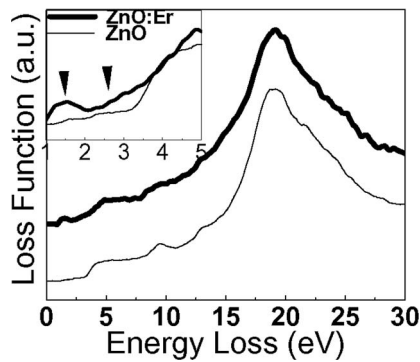


FIG. 3. Loss functions of the as-synthesized and Er doped ZnO nanowires, processed from the corresponding energy loss spectra. Their low energy loss regions are enlarged in the inset for comparison.

oxygen annealing, in contrast to the obvious change of the green emission in the corresponding CL spectra. These experimental facts suggest the non-oxygen-defect related origin of such midgap state(s). It is also interesting to note that the  $\sim 1.4$  eV midgap states are only detectable in some locations on the ZnO nanowire, while the band tail state(s) are(is) commonly observed in all locations examined.

Room temperature  $1.54 \mu\text{m}$  emission is observed in the oxygen annealed nanowire sample under the 325 nm laser excitation (Fig. 4). The Er emission mechanism under indirect excitation is generally explained using an energy transfer model.<sup>5</sup> In the thin film and/or bulk counterparts of Er doped ZnO, the necessity of oxygen annealing to obtain the  $1.54 \mu\text{m}$  luminescence is explained by Er site activation. It has been found that the higher order O coordination around the Er decreased the  $1.54 \mu\text{m}$  PL intensity, which could be significantly improved when the local structure of the Er-O cluster changed to a pseudo-octahedron with  $C_{4v}$  symmetry.<sup>19</sup>

The presence of the ZnO native defects with energy ranging from  $\sim 2$  eV to the ZnO band edge shall have two opposite effects on the  $1.54 \mu\text{m}$  luminescence. On the one hand, they serve as the band tail states that can be pumped by the laser excitations (including the 442 nm excitation). The absorbed energy can then be transferred to the Er ions and leads to the  $1.54 \mu\text{m}$  luminescence. On the other hand, the native defect-related state(s) also affect(s) the efficiency of the  $1.54 \mu\text{m}$  emission, when considering these emissions (the ZnO band edge emission, deep level green emission, and the Er emissions) that are competing with each other. In addition, some of the ZnO native defects serve as nonradiative recombination centers, leading to the quench of the luminescence.

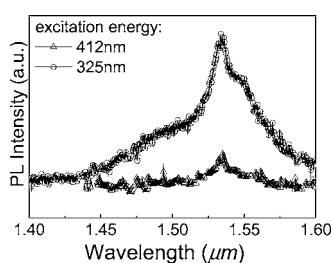


FIG. 4. Photoluminescence spectra taken from the Er doped ZnO nanowires (after annealing) under excitation energies of 325 and 442 nm, respectively.

The observation of the  $1.54 \mu\text{m}$  emission from the annealed nanowires [Fig. 4] under the 442 nm laser excitation is a bit surprising, as such pumping energy is neither above the band gap threshold of ZnO nor close to any energies corresponding to the Er atomic level transitions. In principle, the  $1.54 \mu\text{m}$  would not occur under such a condition due to the lack of effective excitation of the Er electrons. Nevertheless, one shall note that abundant defect state(s) (with energy ranging from 1.4 eV to the ZnO band edge) exist(s) in the band gap of ZnO upon Er implantation, as suggested by both the CL spectra and the EELS data. These defect states could also serve as the energy transfer media for the Er ion excitation, for any pumping energy higher than 1.4 eV.

In conclusion, Er doping into ZnO nanowires is achieved via controlled ion implantation process. We demonstrate that the doped nanowires retain their high microstructural quality with experimental evidence of Er ions taking the substitutional sites of the host lattice. While the O-related defects induced by the ion implantation process are partially recoverable upon oxygen annealing, midgap state(s) generated in the band structure of the ZnO appear(s) to be insensitive to the postimplantation treatment. The high structure quality of the Er doped nanowires and the room temperature  $1.54 \mu\text{m}$  luminescence make them promising candidate to serve as functional units for applications in future optical communications.

This work is supported by a grant from the German Academic Exchange Service and the Research Grants Council of the Hong Kong Joint Research Scheme (Project No. G\_HK013/05). The Tecnai STEM is supported by the National Science Council of Taiwan through Grant No. NSC94-2120-M-002-008.

- <sup>1</sup>Y. N. Xia, P. D. Yang, Y. G. Sun, Y. Y. Wu, B. Mayers, B. Gates, Y. Yin, F. Kim, and H. Yan, *Adv. Mater.* (Weinheim, Ger.) **15**, 353 (2003).
- <sup>2</sup>L. Krusin-Elbaum, D. M. Newns, H. Zeng, V. Derycke, J. Z. Sun, and R. Sandstrom, *Nature* (London) **431**, 672 (2004).
- <sup>3</sup>D. Mihailovic, Z. Jaglicic, D. Arcon, A. Mrzel, A. Zorko, M. Remskar, V. V. Kabanov, R. Dominko, M. Gaberscek, C. J. Gómez-García, J. M. Martínez-Agudo, and E. Coronado, *Phys. Rev. Lett.* **90**, 146401 (2003).
- <sup>4</sup>C. Yang, Z. Zhong, and C. M. Lieber, *Science* **310**, 1304 (2005).
- <sup>5</sup>A. Polman, *J. Appl. Phys.* **82**, 1 (1997).
- <sup>6</sup>K. Takahei and A. Taguchi, *J. Appl. Phys.* **74**, 1979 (1993).
- <sup>7</sup>Z. Zhou, T. Komori, T. Ayukawa, H. Yukawa, M. Morinaga, A. Koizumi, and Y. Takeda, *Appl. Phys. Lett.* **87**, 091109 (2005).
- <sup>8</sup>T. Fukudome, A. Kaminaka, H. Isshiki, R. Satio, S. Yugo, and T. Kimura, *Nucl. Instrum. Methods Phys. Res. B* **206**, 287 (2003).
- <sup>9</sup>S. Komuro, T. Katsumata, T. Morikawa, X. Zhao, H. Isshiki, and Y. Aoyagi, *Appl. Phys. Lett.* **76**, 3935 (2000).
- <sup>10</sup>X. Zhao, S. Komuro, H. Isshiki, Y. Aoyagi, and T. Sugano, *J. Lumin.* **87-89**, 1254 (2000).
- <sup>11</sup>Q. Li and C. R. Wang, *Appl. Phys. Lett.* **83**, 359 (2003).
- <sup>12</sup>D. H. Chen, S. P. Wong, W. Y. Cheung, W. Wu, E. Z. Luo, J. B. Xu, I. H. Wilson, and R. W. M. Kwok, *Appl. Phys. Lett.* **72**, 1926 (1998).
- <sup>13</sup>J. Daniels, C. V. Festenberg, H. Reather, and K. Zeppenfeld, *Springer Tracks in Modern Physics* (Springer, Berlin, 1970), Vol. 54, p. 77.
- <sup>14</sup>R. F. Egerton, *Electron Energy Loss Spectroscopy in the Electron Microscope*, 2nd ed. (Plenum, New York, 1996), p. 245.
- <sup>15</sup>U. Kaiser, D. A. Muller, J. L. Grazul, A. Chuvilin, and M. Kawasaki, *Nat. Mater.* **1**, 102 (2002).
- <sup>16</sup>K. Vanheusden, C. H. Seager, W. L. Warren, D. R. Tallant, and J. A. Voigt, *Appl. Phys. Lett.* **68**, 403 (1996).
- <sup>17</sup>R. L. Hengehold, R. J. Almassy, and F. L. Pedrotti, *Phys. Rev. B* **1**, 4784 (1970).
- <sup>18</sup>J. Wang, X. P. An, Q. Li, and R. F. Egerton, *Appl. Phys. Lett.* **86**, 201911 (2005).
- <sup>19</sup>M. Ishii, S. Komuro, T. Morikawa, and Y. Aoyagi, *J. Appl. Phys.* **89**, 3679 (2001).